Journal of Constructional Steel Research 130 (2017) 120–130

Contents lists available at ScienceDirect

Journal of Constructional Steel Research

On the gradient of the yield plateau in structural carbon steels

Adam J. Sadowski [a,*], J. Michael Rotter [a], Peter J. Stafford [a], Thomas Reinke [b], Thomas Ummenhofer [c]

[a] Department of Civil and Environmental Engineering, Imperial College London, UK
[b] Krebs + Kiefer Ingenieure GmbH, Karlsruhe, Germany
[c] Versuchsanstalt für Stahl, Holz und Steine, Karslruhe Institute of Technology, Germany

ARTICLE INFO

Article history:
Received 11 October 2016
Received in revised form 25 November 2016
Accepted 26 November 2016
Available online 18 December 2016

Keywords:
Structural carbon steel
Stress-strain curve
Yield plateau
Strain hardening
Statistical significance
Linear regression
Full plastic condition

ABSTRACT

New design methodologies are being developed to allow stocky steel members to attain and exceed the full plastic condition. For theoretical validation, such methods require a characterisation of the uniaxial stress-strain behaviour of structural steel beyond an idealised elastic-plastic representation. However, the strain hardening properties of carbon steels are not currently guaranteed by the standards or by any steel manufacturer. Assumptions must thus be made on what values of these properties are appropriate, often based on limited information in the form of individual stress-strain curves. There is very little consistency in the choices made.

This paper first illustrates, using an example elastic-plastic finite element calculation, that a stocky tubular structure can attain the full plastic condition at slendernesses comparable with those defined in current standards and supported by experiment when using only a very modest level of strain hardening, initiated at first yield. It is then hypothesised that the yield plateau in the stress-strain curve for structural carbon steels, classically treated as flat and with zero tangent modulus, actually has a small but statistically significant positive finite gradient. Finally, a robust set of linear regression analyses of yield plateau gradients extracted from 225 tensile tests appears to support this hypothesis, finding that the plateau gradient is of the order of 0.3% of the initial elastic modulus, consistent with what the finite element example suggests is sufficient to reproduce the full plastic condition at experimentally-supported slendernesses.

1. Introduction

It has long been recognised that the full plastic moment of a cross-section cannot be attained at finite strains when assuming an ideal elastic-plastic representation of the stress-strain relation for the steel [1]. It is also very well established that tests on structural members show the reliable exceedance of the full plastic condition at finite slendernesses. In the past, this mismatch was frequently brushed aside by engineers because the focus was on the strength of single structural members for which test evidence was deemed sufficient and empirical rules based on member tests were used in design. However, in the modern world of innovative and complex structural forms, powerful software and limited budgets for testing, it is imperative that new design rules can be devised based principally on computational studies requiring only a minimum of empirical calibration. For this purpose, a reliable and safe characterisation of the post-yield material behaviour is essential. This paper seeks to establish such a characterisation.

Recent years have also seen the development of new design methodologies for steel structures such as the Generalised Capacity Curve [2–4], Reference Resistance Design [5,6] and the Continuous Strength Method [7,8] which formally permit the full plastic resistance of a structure to be attained and exceeded. Their development is based on significant advances in computational modelling that can now treat great structural and material complexities. However, to become an effective and widespread design tool, any such new methodology requires reliable knowledge of the post-yield strain hardening characteristics of the material. Unfortunately, these properties are seldom known with certainty, are not defined in any structural steel materials standard and are not guaranteed by any steel manufacturer.

A further consideration in the definition of the stress-strain relationship to be used for computational modelling is the issue of possible differences between results of a tensile control test and the behaviour of the steel in the structure. First, it is classically assumed that the tensile test also represents the compressive behaviour, which is more important because the structural behaviour for steel structures is dominated by stability considerations. Second, the tensile test, with its accurately machined boundaries, is free of the minor imperfections and variations in real structures that could well trigger the onset of Lüders bands and local yielding, preceding a more general yield state at a slightly higher mean stress. There are thus reasons to believe that the tensile test provides a conservative assessment of the material modelling that should be used for the best assessment of complete structures.

* Corresponding author at: Imperial College London, Skempton Building, South Kensington Campus, London SW72AZ, UK.
E-mail address: a.sadowski@imperial.ac.uk (A.J. Sadowski).

http://dx.doi.org/10.1016/j.jcsr.2016.11.024

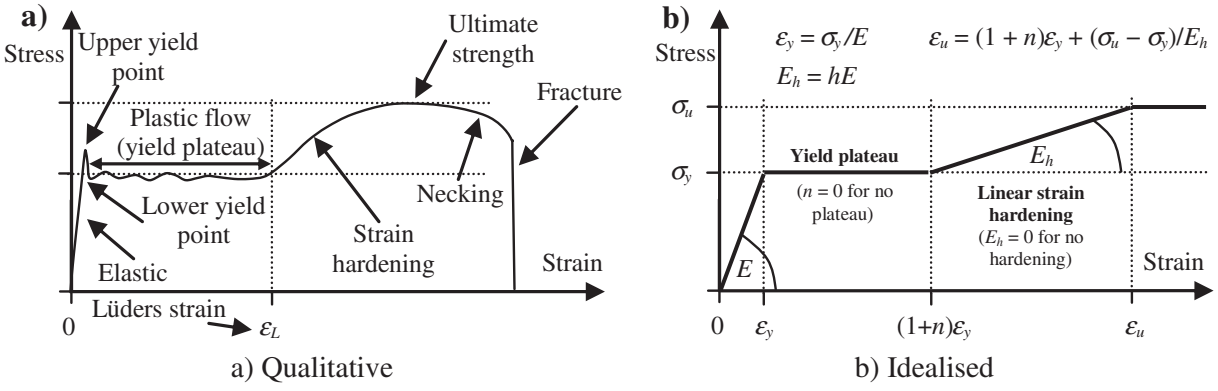

Fig. 1. Classic characterisations of a typical engineering stress-strain curve for structural carbon steel (after Sadowski et al. [16]).

There are many creative and innovative developments in the field of steel structures, with most involving structural systems rather than single structural elements, and the issues of ductility and stability being critical. In the past, the experimental testing of steel structures has relied heavily on single elements, transformed into design rules by statistically based empirical treatments and the results assumed to apply to complete structural systems. But testing is expensive, many different parameters affect the behaviour and the statistical treatment requires many 'identical' tests, so economy demands that computational modelling can be used instead to provide a safe justification. But such modelling is only safe if the material characterisation can safely and reliably define the early post-yield behaviour of the steel, since the competing demands of ductility and economy very commonly lead to small strain stability conditions. This forward-looking perspective is the key driver that led to the present study.

The engineering tensile stress-strain curve for structural carbon steels is classically characterised by three distinct regions. The first is linear elastic until to the upper yield point (Fig. 1a). After a small drop in stress to a 'lower yield' value, straining continues along a 'yield plateau' of plastic flow without any apparent change in stress: Lüders bands of plastic deformation propagate through the specimen [9,10]. When the whole specimen reaches the Lüders strain ε_L, further straining causes the stress to rise (strain hardening) and finally attains a maximum value (the ultimate tensile stress σ_u), after which necking leads to fracture. The length of the yield plateau depends on the manufacturing process and the strain history of the steel and is not an intrinsic material property. Its length is known to depend on the chemical composition, heat treatment, grain size and strain ageing, as well as on the test conditions of loading rate, specimen alignment and stiffness of the test rig [9,11].

The stress-strain relationship has usually been simplified into an idealised piecewise-linear form (Fig. 1b), following one of three variants. The classical 'perfect elastic-plastic' variant requires only two material parameters, the nominal elastic modulus E_{nom} and the yield stress σ_y, and completely ignores strain hardening with a plateau tangent modulus $E_h = 0$ and an infinite yield plateau ($n \to \infty$). The second variant ignores the yield plateau ($n = 0$) but assumes that linear strain hardening E_h begins at the first yield strain $\varepsilon_y = \sigma_y / E_{nom}$, with the stress rising to the ultimate tensile strength σ_u. The value of E_h when $n = 0$ is open to debate, though 1% of the nominal elastic modulus E_{nom} is proposed by the Eurocode on plated structures EN 1993-1-5 [12]. The third variant is like the second but includes a finite-length yield plateau whose length n has been suggested to be up to 15 times ε_y (perhaps 1.5% strain) with E_h tangent moduli anywhere between 0.3% and 4% [13–15].

2. Scope of the present study

As was argued in an earlier study by the authors [16], very little evidence is usually offered by the structural analyst for a particular choice of material model, and this is reflected in a widespread inconsistency

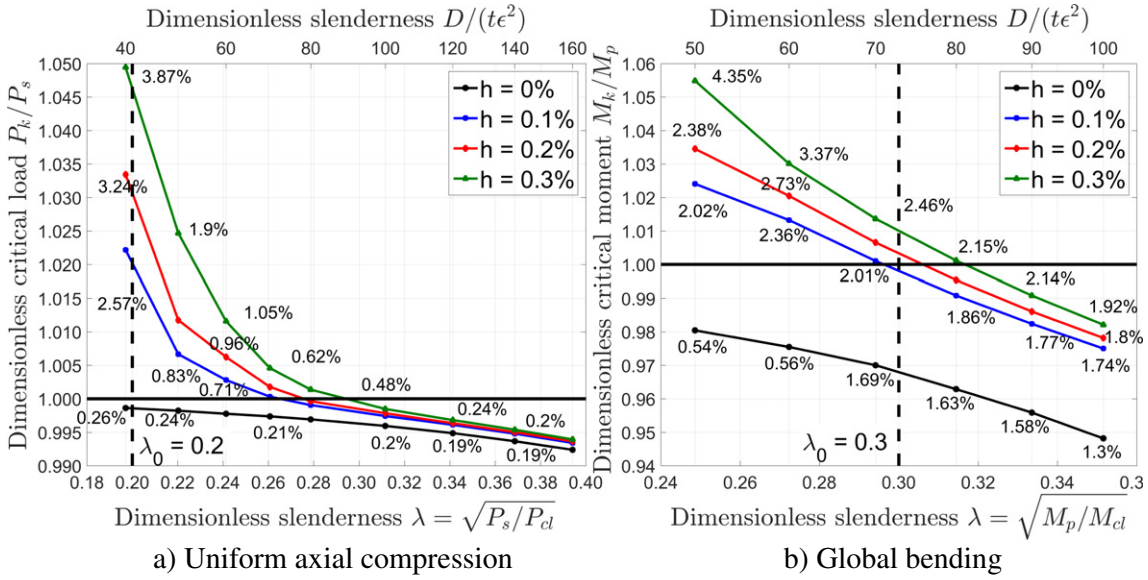

Fig. 2. The extreme stocky zone of capacity curves for perfect hollow circular tubes (Values in % denote the maximum compressive axial strain at the buckling load.).

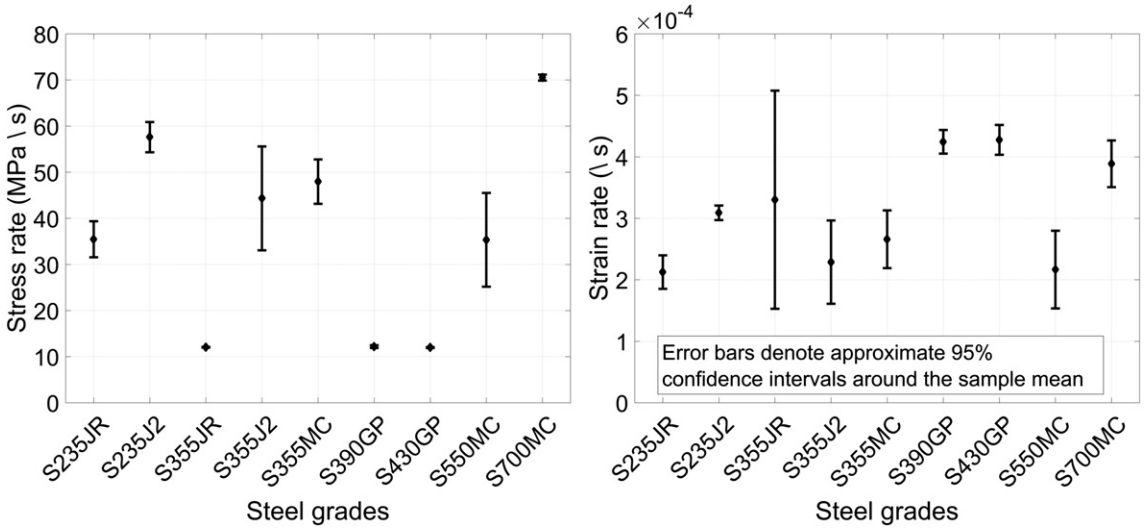

Fig. 3. Numerically-extracted averaged stress and strain rates for each steel grade in the final accepted data set.

between the choices made. It is additionally argued here that where a flat yield plateau is omitted from the material model, unconservative amounts of strain hardening may be assumed to begin at first yield that may overpredict both the true plastified resistance of a structure and the slenderness at which the full plastic resistance can be attained. By contrast, where a yield plateau is included in the material model, it is often assigned a zero gradient so that quite high levels of strain must be attained before the onset of strain hardening. Using such a model, the strain required for hardening may even exceed 5% [9,16], unattainable in any but the stockiest of sections. Given this uncertainty, it is difficult to imagine more advanced design methodologies gaining acceptance without accompanying progress in the characterisation of the post-yield properties of the steel.

A simple parametric finite element analysis is used here to briefly illustrate this point. The buckling resistances of hollow circular structural steel sections with different diameter to thickness ratios are analysed under both uniform axial compression and global bending using a non-linear elastic-plastic treatment with varying levels of linear strain hardening (Fig. 2). These were performed with ABAQUS 6.14-2 [17] using the fully-integrated thick-shell S4 element, with model details, boundary conditions and loading as described by Sadowski and Rotter [18]. The analyses assume a generic S235 steel grade (nominal σ_y = 235 MPa and σ_u = 360 MPa; E_{nom} = 205 GPa and $\nu = 0.3$) with simple linear post-yield strain hardening ($n = 0$) ranging from $h = E_h / E_{nom}$ = 0% (ideal elastic-plastic) up to $h = 0.3\%$ (Fig. 1b). Apart from $h = 0\%$, the yield plateau is defined with a small positive tangent modulus. The tube length was maintained at $14.14\sqrt{(Dt)}$, where D and t are the diameter and thickness respectively, to keep the effect of geometric nonlinearity constant while preventing end boundary effects or ovalisation under bending [19]. The slenderness was varied by changing the D/t ratio. No imperfections were assumed in the model.

Fig. 2 shows the resulting capacity curves in terms of the dimensionless buckling load R_k / R_{pl} against the dimensionless slenderness $\lambda = \sqrt{(R_{pl} / R_{cl})}$, where for uniform axial compression $R_{pl} \equiv P_s$ (squash load) and $R_{cl} \equiv P_{cl}$ (Euler buckling load), while for global bending $R_{pl} \equiv M_{pl}$ (full plastic moment) and $R_{cl} \equiv M_{cl}$ (classical elastic critical moment). The corresponding tube slendernesses are also shown in terms of $D / (t\varepsilon^2)$ where $\varepsilon^2 = 235 / \sigma_y$. First, it is demonstrated that the full plastic condition cannot ever be attained for either load case without strain hardening (for $h = 0\%$, $R_k / R_{pl} \to 1$ from below as $\lambda \to 0$). This reinforces the well-established fact that strain-hardening is essential to reach the simple condition of full plasticity. Secondly, extensive experimental

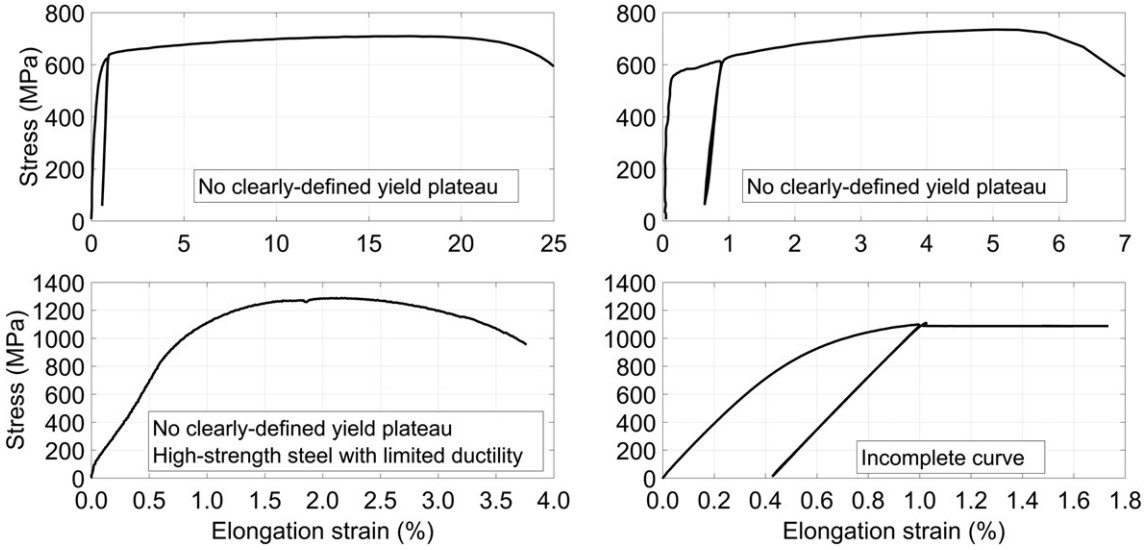

Fig. 4. Examples of stress-strain curves excluded from the final data set.

Table 1
Grade, origin specimen and number of stress-strain curves (total of 225).

Steel grade	○ tube	□ tube	U-section	Sheet	Sheet pile	Wedge	Misc pile	Obs
S235JR	70	7	26	17			6	126
S235J2	6	1					1	8
S355JR	1					1	2	4
S355J2(+N)	11			26			2	39
S355NL				1				1
S355MC	1			6				7
S390GP					6			6
S430GP					8			8
S460ML				2				2
S550MC			1	9		10		20
S700MC				4				4

Table 2
Description of steel grades and numbers according to EN 10027-1 [28] and EN 10027-2 [29].

Steel grade	Steel number	Description
S235JR(H) & S335JR	1.0038 (9) & 1.0045	Charpy impact test with 27 J at 20 °C (JR) Hollow-section (H)
S235J2 & S355J2(+N)	1.0117 & 1.0577	Charpy impact test with 27 J at −20 °C (J2) Normalised (+N)
S355NL	1.0546	Normalised (N); verified minimum impact energy value at −50 °C (L)
S355MC, S550MC & S700MC	1.0976, 1.0986 & 1.8974	Thermomechanically rolled (M) Especially for cold forming (C)
S460ML	1.8838	Thermomechanically rolled (M); verified minimum impact energy value at −50 °C (L)
S390GP & S430GP	1.0522 & 1.0523	Hot rolled sheet pile (GP)

evidence suggests that the full plastic condition is reached at a 'squash limit' slenderness λ_0 of approximately 0.2 for uniform axial compression and 0.3 for global bending [20–22]. It is apparent here that such values of λ_0 are attainable with only very small amounts of strain hardening, of the order of 0.3% of E_{nom} or less, if it is assumed that strain hardening begins immediately after first yield. The effect of including *some* degree of strain hardening is more important than including a large amount of it. Thirdly, the peak compressive axial surface strains appear to be of the order of only ~0.4% and ~2% at the full plastic condition for the two load cases respectively, readily achieved on the 'yield plateau' portion of a typical steel stress-strain curve.

This paper now explores the hypothesis that the tensile yield plateau of mild carbon steel itself exhibits a small but statistically significant, and from a metallurgical perspective plausible, positive gradient corresponding to an effective strain hardening modulus of approximately 0.3% of the initial elastic modulus. Even this small amount of post-yield strain hardening has significant implications for design, as it permits stocky members to attain the full plastic condition at realistic levels of deformation (Fig. 2). To this end, the present study directly extends a previous analysis by the authors [16] which investigated the statistical relationships between the post-yield material properties of three common structural steel grades and offered bounds and confidence intervals for n and h, apparently for the first published time. An extended data set of 225 stress-strain curves is examined here using a multi-part form with an inclined yield plateau. The magnitude and statistical significance of the plateau tangent modulus are explored using a robust series of linear regression analyses.

3. Processing of tensile test measurements

A larger data set than that of Sadowski et al. [16] is studied here with an enhanced functional form to characterise each stress-strain curve in a manner permitting the yield plateau to have a finite gradient. The tensile tests used were conducted for commercial purposes between 2010 and 2013 at the laboratory of the Research Centre for Steel, Timber and Masonry (*Versuchsanstalt für Stahl, Holz und Steine*) at the Karlsruhe Institute of Technology, Germany and followed 'Method B' of ISO 6892-1 [23]. The average stress and strain rates for the tensile tests are illustrated in Fig. 3 and do not exceed 70 MPa/s and 7×10^{-4}/s, which are acceptable bounds for a 'quasi-static' test.

A careful selection procedure was applied so that only those stress-strain curves that exhibited the characteristics of mild carbon steel were accepted (Fig. 1a) into the final data set. Curves that did not exhibit a clearly-defined yield plateau or were from high-strength steel specimens were excluded, and examples of curves that failed this screening are shown in Fig. 4. The resulting data set contained 225 stress-strain curves from a wide selection of nominal grades and origin specimens, with varying degrees of representation, as summarised in Tables 1 and 2. For compactness, specimens with steel grades S235JRH and S235JRG2 were grouped under S235JR, and those with S355J2G3, S355J2H and S355J2+N were grouped under S355J2. It should be added that 70 coupons originated from circular hollow sections ('○ tube' in Table 1) and thus were slightly curved, while the remaining coupons were flat. The authors' previous study [16] showed that the additional cold forming to which the curved coupons were subject has a negligible effect on the strength but potentially a detrimental effect on the ductility. However, this aspect will not be considered further in this study.

The numerical properties of the stress-strain curves were considered at 'face value' and the derived quantities should be viewed with a degree of caution. Though perhaps an unconventional approach, it should be kept in mind that modern finite element predictions of structural resistances of various members and components are routinely based on measured individual stress-strain curves, or idealised simplifications thereof, fed directly into the software (e.g. [24–26]), thus the 'face value' of this information already plays a central role in current research. Even less information is typically available in design, with reliance placed on nominal values. The authors stress that the chief aim of this paper is to raise awareness and stimulate discussion, rather than to produce definitive characterisations of these steels. The data used herein, though invaluable, was not gathered for research purposes and was released for analysis on a strictly 'as is' basis.

Lastly, for many of the S235 and S355 specimens in this data set the authors' previous study [16] identified significant inconsistencies between the nominal and actual yield and ultimate stress values. This is directly attributable to the widespread practice of selling higher grade steel as a lower grade, where either a batch of steel is deemed to fail quality control [27] or stockists lack particular sections in the specified grade. The authors had no choice but to accept the nominal designations, and though the practice is justifiable economically it unfortunately leads to inhomogeneous data for research purposes, with a significant scatter caused by systematic 'errors'.

Table 3
Functional forms to characterise the stress-strain curves of structural steels with a yield plateau, after Sadowski et al. [16,30].

Stress	Flat yield plateau	Inclined yield plateau	Strain ranges
$\sigma(\varepsilon)=$	Discarded as unnecessary		$\varepsilon < \varepsilon_y$
	Constant in ε: σ_y	Linear in ε: $\sigma_{y,l} + (\sigma_{y,l} - \sigma_{y,u})(\varepsilon - \varepsilon_y) / (\varepsilon_n - \varepsilon_y)$	$\varepsilon_y \le \varepsilon < \varepsilon_n$
	Septic in ε: $a_0 + a_1(\varepsilon - \varepsilon_n) + \ldots + a_7(\varepsilon - \varepsilon_n)^7$		$\varepsilon \ge \varepsilon_n$

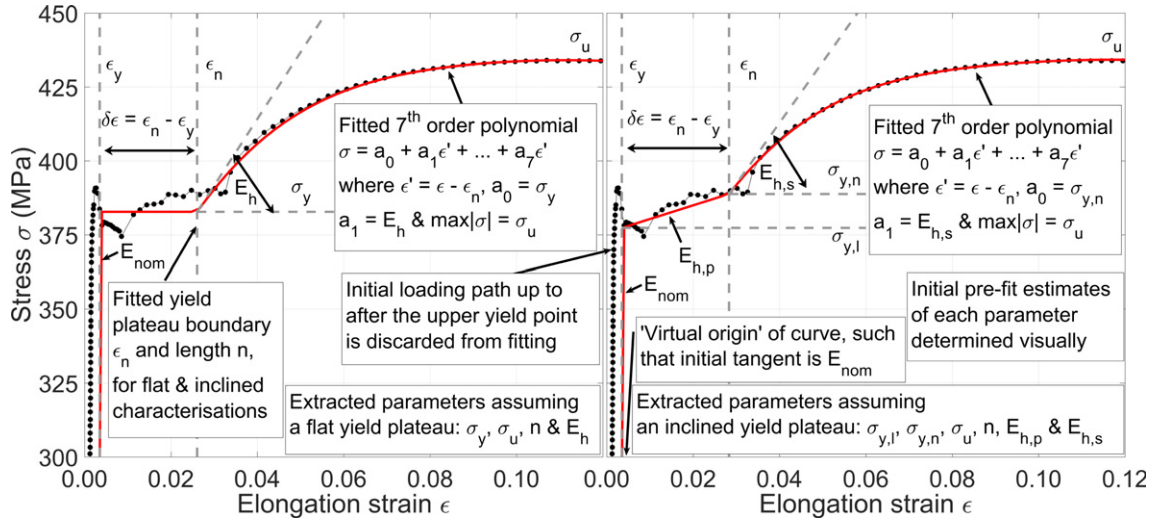

Fig. 5. Sample measured stress-strain curves and their characterisation.

4. Curve fitting methodology

4.1. Previous treatment

The precursor study [16] employed a two-part functional form to characterise the full 'post-yield' portion of the stress-strain curves from 174 structural steel samples tested in tension. Significant nonlinearities were often found in the initial 'pre-yield' portion of many of the curves, attributed to slipping of the clamped specimen during testing, prior straightening, minor misalignment or elastic deformations in the test rig. As these deformations are inconsistent with a strict linear elastic treatment of this region, and since the focus of this study is on the post-yield materials properties only, the data in this portion was discarded (Table 3). The measured strain at which the plateau begins was identified by careful visual inspection (Fig. 5a), and this point was then identified as the yield strain, defined as $\varepsilon_y = \sigma_y / E_{nom}$ where $E_{nom} = 205$ GPa giving a numerical 'offset' to all later measurements. Since all strain-based material variables considered here are related to strain differences rather than absolute values, this adjustment had no impact on the later conclusions. Where a measured curve had a clear upper yield point, a small part of the data relating to it was discarded to avoid bias by this locally high value. Consistent with a classical treatment, the yield plateau was then assumed to be flat at σ_y until a strain ε_n, both determined by least-squares curve fitting. Finally, the curved portion of the curve corresponding to strain hardening and necking was characterised by a 7th order polynomial (septic) $\sigma = a_0 + a_1(\varepsilon - \varepsilon_n) + \ldots + a_7(\varepsilon - \varepsilon_n)^7$, where $a_0 \equiv \sigma_y$ is the constant plateau yield stress to provide continuity and $a_1 \equiv E_h$ is the strain hardening initial tangent modulus. The high order of this functional form was chosen solely to provide a very accurate representation of the initial tangent E_h near ε_n, and it is not suggested here that this portion of the curve actually follows such a polynomial relationship.

A related separate study was conducted on the post-yield material properties of spirally-welded structural steel tubes [30] to explore the effect of specimen orientation on the assumed isotropy in these anisotropically formed tubes. This used a similar characterisation, but with a finite slope on the yield plateau (Fig. 5b). This treatment was chosen because the 28 curves in that data set were found to systematically exhibit yield plateaus with tangent moduli up to ~1.5% of the nominal elastic modulus $E_{nom} = 205$ GPa, and the simple assumption of a flat yield plateau was clearly incorrect. The reason for the high slope in these tests was never fully identified, but it could be attributed to the spiral manufacturing process (see, for example, van Es et al. [31]).

4.2. Present characterisation

A modified version of the extended 'inclined yield plateau' characterisation (Fig. 5b, Table 3) was adopted here to determine whether the full 225 curves exhibit yield plateaus with statistically significant non-zero gradients. The chosen functional form enabled the extraction of yield stress values $\sigma_{y,l}$ and $\sigma_{y,n}$ corresponding to the beginning and end of the yield plateau (these are not 'yield points' in the metallurgical sense) defined at the reduced strain values of ε_y and ε_n respectively. The tangent modulus of the inclined yield plateau can then be obtained as $E_{h,p} = (\sigma_{y,n} - \sigma_{y,l}) / (\varepsilon_n - \varepsilon_y)$. The dimensionless length of the plateau was defined as $n = \delta\varepsilon / \varepsilon_y = (\varepsilon_n - \varepsilon_y) / \varepsilon_y$, where ε_y is the deduced first yield strain $\sigma_{y,l} / E_{nom}$. The initial tangent modulus $E_{h,s}$ of the true strain hardening region beyond ε_n was again found as the linear coefficient of the fitted septic polynomial. Both hardening tangent moduli were normalised by E_{nom} (expressed as a percentage for convenience): $h_p = E_{h,p} / E_{nom}$ and $h_s = E_{h,s} / E_{nom}$. No constraint was placed on the sign of $E_{h,p}$ during fitting. In the context of safe structural design, it should be recognised that a low value of n and a high value of h_s ensure a strong post-plastic structural behaviour, while a high n and low h_s signal that caution should be exercised in assuming that the plastic resistance can be reached. Further details of the fitting procedure and an explanation of the adoption of E_{nom} in place of the measured elastic moduli are given in Sadowski et al. [16]. All data processing was performed here using the Matlab R2014a [32] programming environment. The statistical significance of a yield plateau gradient, whether positive or negative, was investigated using regression analyses.

5. Descriptive statistics

Descriptive statistics for a subset of this data (120 S235JR, 31 S355J2+N and 23 S550MC specimens) were previously analysed adopting the flat plateau (Fig. 5a) and published in Sadowski et al. [16] where the relationships between the post-yield parameters were also extensively explored. Here a larger data set is used, with additional steel grades, and using the inclined yield plateau characterisation (Fig. 5b). The global statistics for each of the five independent material variables $\sigma_{y,l}$, σ_u, h_p, n and h_s are presented in Table 4 where the mean, characteristic (5th or 95th percentiles of a normal distribution for unfavourable values, depending on the variable), minimum, maximum, nominal (for σ_y and σ_u), standard error (SE), coefficient of variation (CV – expressed as a percentage),

Table 4
Summary statistics of the full data set (222 curves, 3 excluded).

	S235JR (obs = 126)					S235J2 (obs = 8)*					S355JR (obs = 4)*				
	$\sigma_{y,l}$ *MPa*	σ_u *MPa*	n	h_p *(%)*	h_s *(%)*	$\sigma_{y,l}$ *MPa*	σ_u *MPa*	n	h_p *(%)*	h_s *(%)*	$\sigma_{y,l}$ *MPa*	σ_u *MPa*	n	h_p *(%)*	h_s *(%)*
Mean	404.9	470.1	13.4	0.15	1.07	405.5	464.5	11.5	0.09	0.91	397.3	546.9	9.0	0.23	2.42
Characteristic†	315.2	393.3	24.4	-1e-3	0.32	375.3	417.7	15.1	-6e-3	0.36	338.6	525.3	17.6	-3e-3	1.64
Min.	275.7	331.2	0.9	-0.05	0.04	375.3	417.7	6.8	-6e-3	0.36	338.6	525.3	4.8	-3e-3	1.64
Max.	577.9	620.9	31.8	0.94	2.91	429.9	520.1	15.1	0.16	1.96	425.3	568.5	17.6	0.38	2.73
Nominal	235	360	*n/a*	*n/a*	*n/a*	235	360	*n/a*	*n/a*	*n/a*	355	470	*n/a*	*n/a*	*n/a*
St.Dev.	51.0	52.4	6.1	0.12	0.48	17.1	32.3	3.1	0.06	0.49	40.3	23.9	5.9	0.17	0.52
Se	4.54	4.67	0.54	0.01	0.04	6.04	11.43	1.09	0.02	0.17	20.12	12.00	2.97	0.09	0.26
Cv (%)	12.6	11.2	45.3	81.2	45.4	4.2	7.0	26.8	69.6	53.7	10.1	4.4	66.3	77.1	21.5
Skew	0.26	0.49	0.68	2.55	0.99	-0.29	0.32	-0.13	-0.80	1.26	-0.98	-2e-4	0.99	-0.49	-1.10
Kurtosis‡	1.47	0.83	0.44	14.17	2.30	0.19	-0.05	-1.37	-0.60	3.17	2.81	-5.94	2.94	-0.76	3.67
	S355J2 (obs = 39)					**S355MC (obs = 7)***					**S390GP (obs = 6)***				
	$\sigma_{y,l}$ *MPa*	σ_u *MPa*	n	h_p *(%)*	h_s *(%)*	$\sigma_{y,l}$ *MPa*	σ_u *MPa*	n	h_p *(%)*	h_s *(%)*	$\sigma_{y,l}$ *MPa*	σ_u *MPa*	n	h_p *(%)*	h_s *(%)*
Mean	406.5	549.6	9.1	0.34	1.97	443.6	483.9	22.3	0.06	0.64	457.6	597.8	7.7	0.07	2.42
Characteristic†	344.3	406.0	31.9	-0.05	0.56	373.0	435.4	28.4	0.01	0.33	444.4	584.4	10.6	0.02	2.31
Min.	331.4	369.8	1.8	-0.06	0.44	373.0	435.4	18.6	0.01	0.33	444.4	584.4	5.0	0.02	2.31
Max.	595.4	669.8	49.1	1.61	3.16	505.2	541.1	28.4	0.13	0.81	475.5	617.4	10.6	0.14	2.57
Nominal	355	470	*n/a*	*n/a*	*n/a*	355	470	*n/a*	*n/a*	*n/a*	390	490	*n/a*	*n/a*	*n/a*
St.Dev.	75.2	57.6	9.4	0.40	0.82	59.6	52.2	3.1	0.05	0.17	13.7	15.0	2.36	0.05	0.12
Se	12.05	9.22	1.50	0.06	0.13	22.54	19.74	1.16	0.02	0.06	5.60	6.13	0.97	0.02	0.05
Cv (%)	18.5	10.5	103.3	116.6	41.4	13.5	10.8	13.8	76.8	26.4	3.0	2.5	30.8	67.0	4.87
Skew	1.43	-1.44	3.07	1.61	-0.62	0.09	0.26	1.08	0.45	-0.79	0.44	0.62	-0.02	0.39	0.31
Kurtosis‡	0.81	3.75	10.87	2.79	-1.06	-2.47	-2.74	3.00	-1.84	0.63	-1.85	-1.85	-1.80	-1.12	-2.34
	S430GP (obs = 8)*					**S550MC (obs = 20)**					**S700MC (obs = 4)***				
	$\sigma_{y,l}$ *MPa*	σ_u *MPa*	n	h_p *(%)*	h_s *(%)*	$\sigma_{y,l}$ *MPa*	σ_u *MPa*	n	h_p *(%)*	h_s *(%)*	$\sigma_{y,l}$ *MPa*	σ_u *MPa*	n	h_p *(%)*	h_s *(%)*
Mean	447.1	591.1	8.1	0.13	2.51	611.8	670.4	8.5	0.16	1.02	747.7	814.4	2.7	0.29	0.64
Characteristic†	431.0	579.7	10.1	0.01	2.37	564.0	625.4	14.2	-0.03	0.46	668.1	740.7	3.6	0.20	0.56
Min.	431.0	579.7	5.2	0.01	2.37	558.2	621.6	1.1	-0.04	0.36	668.1	740.7	1.6	0.20	0.56
Max.	466.4	610.1	10.1	0.37	2.65	661.6	765.9	14.9	0.61	2.64	780.1	840.8	3.6	0.40	0.76
Nominal	430	510	*n/a*	*n/a*	*n/a*	550	600	*n/a*	*n/a*	*n/a*	700	750	*n/a*	*n/a*	*n/a*
St.Dev.	10.6	11.1	1.7	0.12	0.11	27.8	39.1	3.66	0.20	0.58	53.3	49.2	0.93	0.09	0.09
Se	3.76	3.92	0.60	0.04	0.04	6.21	8.75	0.82	0.05	0.13	26.6	24.6	0.46	0.05	0.04
Cv (%)	2.4	1.9	21.1	94.7	4.3	4.5	5.8	43.0	127.1	57.0	7.1	6.0	34.7	32.4	13.4
Skew	0.38	0.51	-0.42	1.21	0.12	-0.25	0.86	-0.07	1.09	1.95	-1.13	-1.16	-0.12	0.13	0.74
Kurtosis‡	0.76	-0.90	-0.72	2.54	-1.42	-0.49	0.34	-0.37	0.38	4.16	3.87	3.99	-3.09	-3.48	2.45

† 5th %-ile for $\sigma_{y,l}$, σ_u, h_p and h_s; 95th %-ile for n; ‡ excess value; * small sample, treat with care;

skewness and *excess* kurtosis are shown. Some of this data is also shown in Figs. 6 and 7 as a function of the steel grade, with error bars to show 95% confidence intervals around the sample means (denoting the limits where the true population means may be said to be found with 95% confidence). The grades shown are only for those represented by four or more specimens, though any statistics

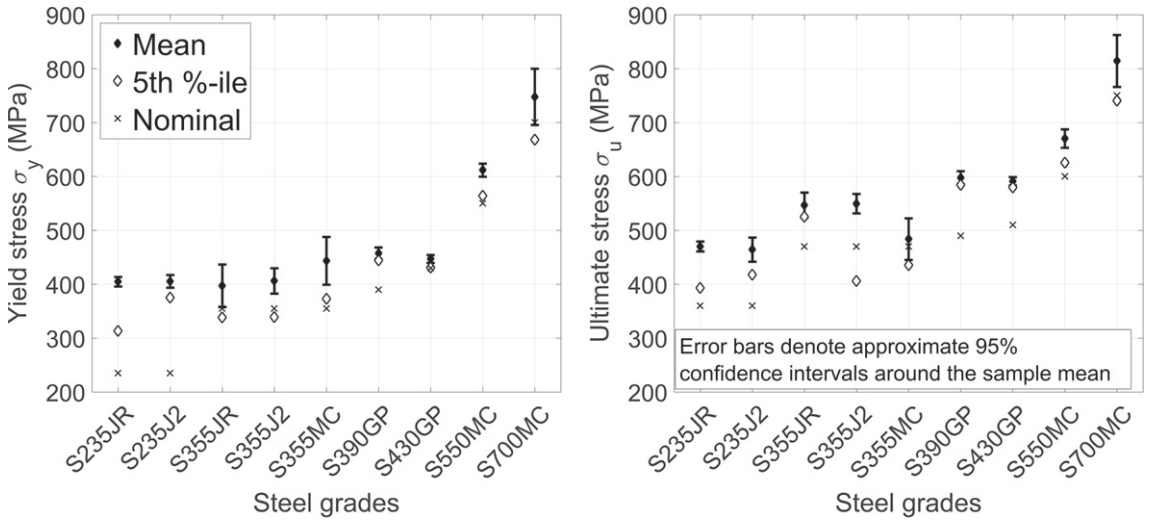

a) Yield stress σ_y b) Ultimate stress σ_u

Fig. 6. Line plots by steel grade of mean, characteristic (estimated 5th %-ile) and nominal (min. specified) key stresses, including 95% confidence intervals.

for a grade represented by <10 specimens should be interpreted with care.

The stress variables $\sigma_{y,l}$ and σ_u exhibit smaller SEs and CVs than the strain-related variables n, h_p and h_s. This suggests that strain-related material parameters may be intrinsically more statistically variable than stress-based ones, though it is likely that the difficulty of accurately measuring small strains also plays a role [33]. For the steel grades S235JR and S235J2, the values of n and h_s lie around $n \approx 12$ and $h_s \approx 1\%$. By contrast, the S355J2+N, S390GP and S430GP grades exhibit extensive post-plateau strain hardening ($h_s \approx 2.5\%$) but only a relatively short yield plateau ($n \approx 8$), while the S355MC grade exhibits a very low $h_s \approx 0.8\%$ with an exceptionally high n of 25 so that the ideal elastic-plastic model may be quite accurate. These differences indicate that the strain hardening ratio h_s and the yield plateau length n must be carefully identified for each steel grade: a steel with a long yield plateau may also have a lower level of strain hardening. Similarly, h_s appears to be positively correlated and n negatively correlated with the ultimate stress σ_u. Sadowski et al. [16] presented regression equations for each of these relationships which confirmed these tendencies on the best-represented S235JR grade, with regression coefficients satisfying at least the 95% confidence level (meaning that they were statistically different from zero with at least 95% confidence). The fortuitous presence of such correlations may mean that it may be possible to establish predictive bounds for the relatively unknown variables n and h_s by conditioning the prediction upon specific values of $\sigma_{y,l}$ and σ_u. However, a larger data set is required in order to robustly estimate the appropriate correlation values before such conditional prediction bounds can be used with confidence in practice.

The variable h_p, which represents the tangent modulus of the yield plateau, consistently exhibits a mean value of ~0.1 to 0.3% across every steel grade in the data set. However, h_p also exhibits the highest SEs and CVs of any of the variables, suggesting great scatter in the extracted values and variation from the mean. Aside from intrinsic variability, the high scatter may likely be attributed to insufficient care taken during commercial testing to ensure a carefully-captured yield plateau (the ISO 6892-1 [23] testing procedure does not actually aim

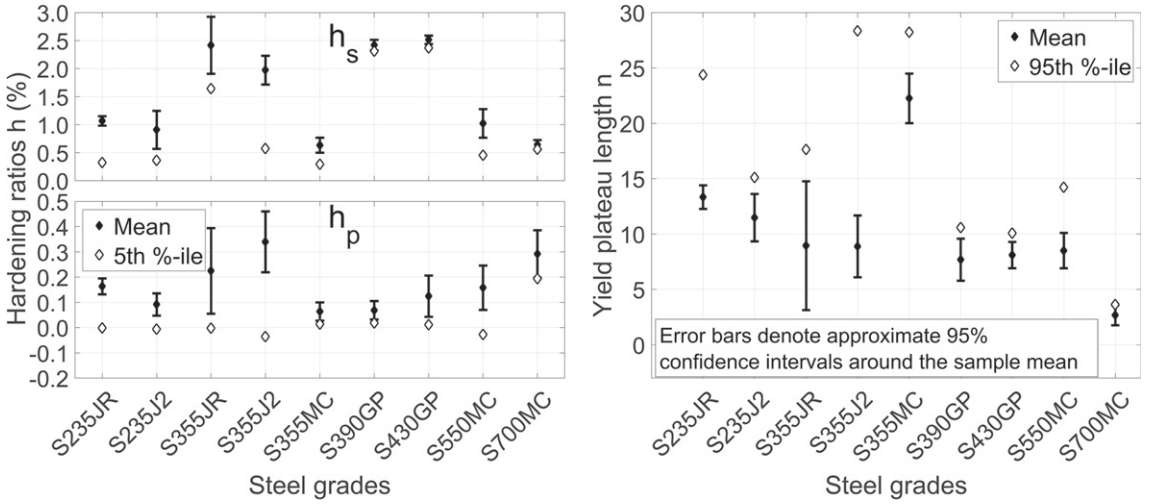

a) Hardening ratios h_p and h_s (%) b) Yield plateau length n

Fig. 7. Line plots by steel grade of mean and characteristic post-yield parameters (estimated 5th %-ile for h and 95th %-ile for n), including 95% confidence intervals.

Table 5
Summary of linear regression analyses of only the yield plateaus exhibiting positive gradients ($a_2 \equiv E_{h,p} > 0$).

Significance level of a_2 coefficient	No. curves (total 195)	Min. h_p %	Max. h_p %	Mean h_p (st. dev.) %	5th %-ile h_p %	Mean r^2 (st. dev.)
0.001 (99.9%)	152	0.01	3.43	0.33(40)[a]	0.04	0.61(26)[a]
0.01 (99%)	11	0.03	1.30	0.42(36)[a]	0.04	0.44(20)[a]
0.05 (95%)	12	0.007	1.56	0.31(44)[a]	0.008	0.29(28)[a]
Not significant	22	0.004	0.57	0.14(17)[a]	0.006	0.10(14)[a]

[a] E.g. 0.33(40) implies a mean of 0.33 and a standard deviation of 0.40.

Table 6
Summary of linear regression analyses of only the yield plateaus exhibiting negative gradients ($a_2 \equiv E_{h,p} < 0$).

Significance level of a_2 coefficient	No. curves (total 30)	Min. h_p %	Max. h_p %	Mean h_p (st. dev.) %	5th %-ile h_p %	Mean r^2 (st. dev.)
0.001 (99.9%)	13	−0.46	−0.03	−0.22(15)	−0.44	0.37(30)
0.01 (99%)	1	*n/a*	*n/a*	−0.09	*n/a*	0.31
0.05 (95%)	3	−0.20	−0.12	−0.16(04)	−0.20	0.20(11)
Not significant	11	−0.60	−0.003	−0.16(18)	−0.59	0.08(10)

to produce a plateau). It is also possible that the unloading and reloading from the plateau to obtain an accurate elastic modulus estimate, which is known to have been performed for 206 of the 225 tests (91.6% of the data set), may have affected the extracted h_p. The highest extracted values of h_p approach 1% and are for the S235JR grade. Elsewhere the highest values are around 0.5%, though one S355J2 specimen displayed an h_p of 1.61%. It is also of interest that some specimens showed a negative slope on the yield plateau ($h_p < 0$), which seems to indicate strain softening and may also be an artefact of the test process. The widespread statistical significance in the plateau gradient values, and a discussion of the proportions of tests that showed positive and negative gradients and whether these may have been affected by the unloading and reloading from the plateau, are explored below using a robust series of regression analyses.

6. Linear regression on the yield plateau alone

6.1. Introduction

The previous analysis furnished a fitted value of the horizontal plateau length n for each of the 225 stress-strain curves. This permits the measured data points associated with the yield plateau to be isolated from the rest of the curve and a more careful ordinary least squares (OLS) linear regression analysis of stress σ against dimensionless strain ε on the yield plateau. The first set of regression analyses assumed the usual linear form:

$$\sigma = a_1 + a_2 \cdot \varepsilon' + \delta \tag{1}$$

where $\varepsilon' = \varepsilon - \varepsilon_y$ ($\varepsilon_y \le \varepsilon \le \varepsilon_n$ with ε_n identified by n from the previous analysis). The intercept a_1 is the lower yield plateau stress $\sigma_{y,l}$ and a_2 is the plateau gradient $E_{h,p}$, with δ as the disturbance or error term. This simple linear model produces slightly different values of $\sigma_{y,l}$ and $E_{h,p}$ from the previous multi-part characterisation, because the regression is unconstrained by continuity requirements with the adjacent portions of the curve. The sign of a_2 could naturally be found as positive or negative. The extracted plateau gradient is again presented in dimensionless form $h_p = E_{hp} / E_{nom}$, where $E_{nom} = 205$ GPa and expressed as a percentage for ease of assimilation. Statistical significance tests performed on the a_2 regression coefficient focus on whether they satisfy 0.05 (95%), 0.01 (99%) and 0.001(99.9%) levels [34]. The a_1 coefficient was found to always be statistically very highly significant, reflecting the obvious fact that the yield stress is never zero.

6.2. Preliminary linear regression statistics

Altogether 195 stress-strain curves (86.7%) were found to have a positive coefficient $a_2 \equiv E_{h,p}$ (Table 5; Fig. 8a). Of these, 152 were very highly significant with $p < 0.001$ (67.6%) and a mean r^2 correlation coefficient of 0.61 (CV = 43%). The mean dimensionless tangent modulus h_p was 0.33% (CV = 122%), although a few individual values in excess of 1% were found. A further 23 plateaus had gradients that were significant at the 99% (11 curves) and 95% (12 curves) levels, with similar mean h_p values of 0.42% (CV = 86%) and 0.17% (CV = 138%) respectively.

Thirty stress-strain curves were found to exhibit a negative coefficient $a_2 \equiv E_{h,p}$ (13.3%), appearing to suggest strain softening on the yield plateau (Fig. 8b; Table 6). However, only 17 of these (7.6%) were statistically significant ($p < 0.05$) with a combined mean h_p of −0.24%

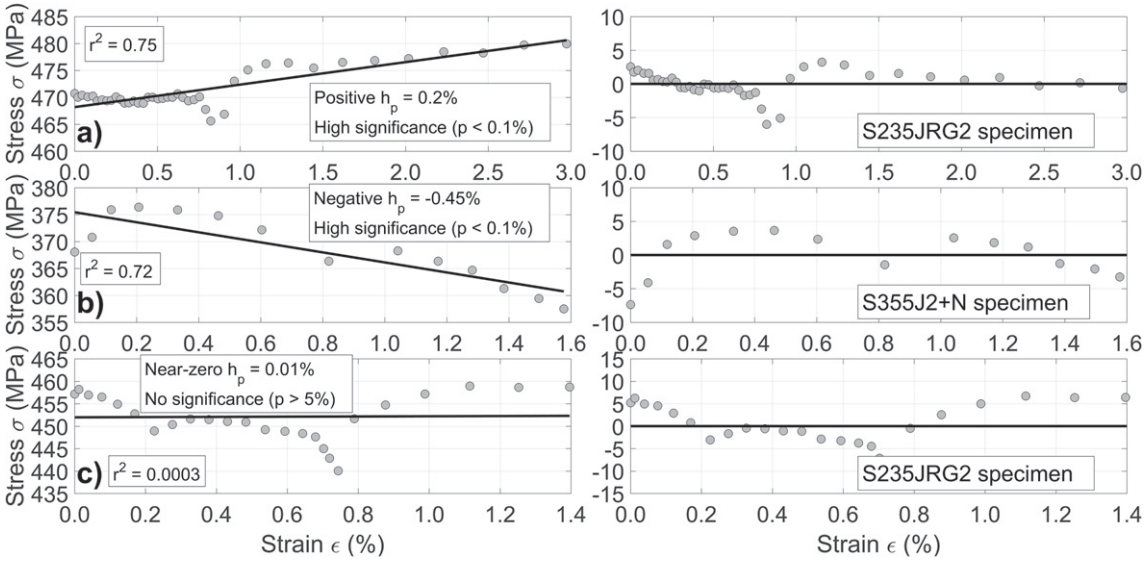

a) Yield plateau linear regressions b) Residuals

Fig. 8. Illustrations of linear regressions on yield plateaus with statistically positive, near-zero and negative gradients, together with residuals.

(CV = 104%), and r^2 coefficients were all very low. This small group of anomalous tests can probably be attributed to the test procedure, but it should serve as a caution to those who perform finite element calculations using parameters calibrated with only a handful of measured stress-strain curves. Only 34 stress-strain curves (15.1%) were found to have no significant plateau gradient of either sign (Fig. 8c).

6.3. Possible influence of autocorrelation

The significance tests carried out above as part of OLS linear regression rely on a number of classical assumptions, one of them being that there is no serial correlation between the error terms δ [35]. When this assumption is violated due to autocorrelation of errors, a distinct possibility given that every data point is dependent on a previous measurement in a stress-strain curve, the classical OLS model may significantly underestimate the standard errors of the regression coefficients and thus overestimate their statistical significance. Indeed, conventional Durbin-Watson and Ljung-Box 'Q' tests [36] tested positive for autocorrelation in 90% of the stress-strain curves. There are a myriad of specialised statistical methods that aim to correct for this effect as part of 'generalised' linear regression methods, much of which lie beyond the scope of this paper. A simpler illustration of the potential sensitivity of the significance tests to standard error inflation is to recalculate the p values using artificially inflated standard errors. Re-estimating each gradient's standard error using a formula which corrects for autocorrelation (Law and Kelton [37]; p. 284), it was found that up to a five-fold inflation may be representative. As shown in Fig. 9 for positive gradients only, while such high variance inflation clearly leads to a less generous portion of curves claiming very high significance of the gradient coefficient and a rise in coefficients that are not at all significant, a majority still satisfies at least 95% significance even at the highest considered level of inflation.

6.4. Possible influence of steel grade

A regression was next performed on a transformed 'centred and scaled' lumped data set. The transformation involves mapping the centroid of the data to the origin and normalising by the standard deviation (Eq. (2a,b)). This has the benefit of permitting a comparison between data defined on different scales and permits all stress-strain curves to be considered simultaneously, while also removing the necessity for an intercept term from the regression equation.

$$\overline{\sigma} = \left(\frac{\sigma - mean(\sigma)}{std(\sigma)}\right) \text{and } \overline{\varepsilon} = \left(\frac{\varepsilon - mean(\varepsilon)}{std(\varepsilon)}\right) \quad (2a, b)$$

A simple global regression was first performed as follows:

$$\overline{\sigma} = b_2 \cdot \overline{\varepsilon} + \delta \quad (3)$$

The coefficient of b_2, a global gradient through the entirety of the data set (Fig. 10), was found to be very highly significant ($p < 0.001$) with a positive value of 0.605. A further analysis was then performed using a more complete regression equation:

$$\begin{aligned}\overline{\sigma} = {} & c_{S235JR} \cdot \overline{\varepsilon} + c_{S235J2} \cdot \alpha_{S235J2} \cdot \overline{\varepsilon} + c_{S355JR} \cdot \alpha_{S355JR} \cdot \overline{\varepsilon} + \ldots \\ & c_{S355J2} \cdot \alpha_{S355J2} \cdot \overline{\varepsilon} + c_{S355MC} \cdot \alpha_{S355MC} \cdot \overline{\varepsilon} + c_{S390GP} \cdot \alpha_{S390GP} \cdot \overline{\varepsilon} + \ldots \\ & c_{S430GP} \cdot \alpha_{S430GP} \cdot \overline{\varepsilon} + c_{S550MC} \cdot \alpha_{S550MC} \cdot \overline{\varepsilon} + c_{S700MC} \cdot \alpha_{S700MC} \cdot \overline{\varepsilon} + \delta\end{aligned} \quad (4)$$

This model considers interactions between the gradient coefficients (the cs) and binary 'dummy' variables (the αs) which are equal to unity if the given data point originates from the subscripted steel grade and zero if otherwise. There are one less 'dummy' variables than the total number of steel grade categories (as defined in Table 4), with the default category (i.e. when all α's are set to zero) corresponding to the best-represented S235JR grade. The statistics of this fit are summarised in Table 7. Unscaled values of the gradients b or c's may easily be recovered via a linear transformation.

The 'default' c_{S235JR} gradient coefficient was found to be 0.616, very highly significant and close to the value of the global gradient $b_2 = 0.605$ obtained using Eq. (3). Further, the enhanced model offers only a negligible reduction in the root mean squared error (RMSE), suggesting that the lumped data set is anyway dominated by the best-represented steel grade, as may be expected. However, the remaining gradient coefficients are also very highly significant (with the exception of only c_{S355J2} and c_{S355MC}), suggesting that the steel grade does indeed influence the magnitude of the yield plateau gradient. Additionally, of the very highly significant c coefficients all but c_{S700MC} were found to be negative, suggesting that those (higher) steel grades on average have a lower yield plateau gradient than S235JR. For the S390GP grade, for example, this would be $c_{S235JR} + c_{S390GP} \cdot \alpha_{S390GP} = 0.616 - 0.358 \cdot 1 = 0.258$, with all other α's being zero. Importantly, none of the c coefficients reduce the yield plateau gradient to zero or below, suggesting that it should always be a positive value.

6.5. Possible influence of unloading and reloading

Finally, the possibility that the apparent gradient of the yield plateau may be an artefact of the practice of unloading and reloading the specimen part way along the plateau to evaluate the elastic modulus was investigated. Fortuitously, 19 of the 126 S235JR specimens did not have this unloading-reloading path: of these, all but one was found to exhibit a positive yield plateau gradient significant at the 99.9% level. A simple

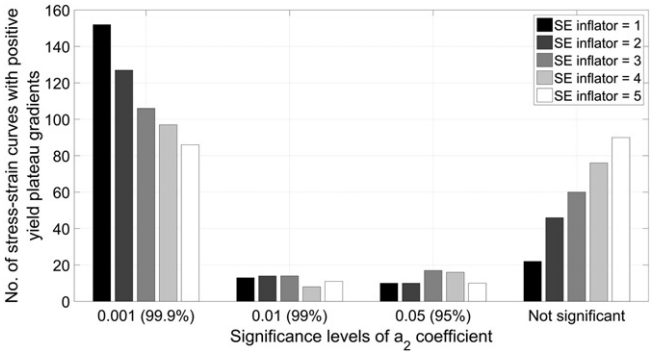

Fig. 9. Potential influence of standard error (SE) inflation on the significance levels of the positive $a_2 \equiv E_{h,p}$ yield plateau gradients.

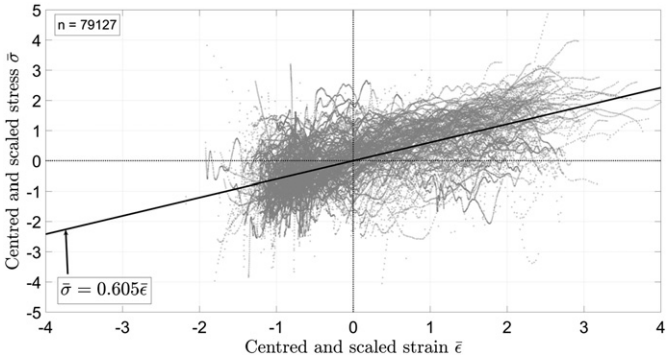

Fig. 10. Regression on the centred and scaled lumped data set of yield plateaus (RMSE = 0.795 and $r^2 = 0.37$).

Table 7
Summary statistics of a linear regression model with interactions and 'dummy' variables on the centred and scaled lumped data (RMSE = 0.794 and $r^2 = 0.37$).

Coefficient	c_{S235JR}	c_{S235J2}	c_{S355JR}	c_{S355J2}	c_{S355MC}	c_{S390GP}	c_{S430GP}	c_{S550MC}	c_{S700MC}
Value	0.616	−0.064	−0.173	0.018	−0.006	−0.358	−0.132	−0.142	0.288
Grade c[a]	0.616	0.552	0.443	0.634	0.610	0.258	0.484	0.474	0.904
p value	<0.001	<0.001	<0.001	0.095	0.678	<0.001	<0.001	<0.001	<0.001
Significance	99.9%	99.9%	99.9%	None	None	99.9%	99.9%	99.9%	99.9%

[a] $c_{S235JR} + c_i$ where i is a grade other than S235JR (for which $c_i = 0$).

comparison is shown in Table 8 of the summary statistics for h_p, r^2 and number of readings on the yield plateau for the two subsets with and without the unloading-reloading path, calculated using the original simple regression model in Eq. (1).

The comparison appears to suggest that the significance of the positive yield plateau gradient persists even in a specimen unaffected by the unloading-reloading path. A simple one-sample t-test performed on both sub-sets using the extracted values of h_p rejects the null hypothesis ($p < 0.001$) that the gradients should be zero. A two-sample t-test of the two sub-sets of extracted h_p values with and without the assumption of equal variances respectively gives $p = 0.123$ and $p = 0.276$, in neither case rejecting the null hypothesis that they both come from the same population. Further, a simple regression of h_p on α, where α is a 'dummy' variable equal to 1 where the curve exhibited an unloading-reloading path and 0 where it did not, and using only those curves with gradients significant at the 99.9% level, results in the equation h_p (%) $= 0.23 - 0.07\alpha$. The negative coefficient for α appears to suggest that the presence of the unloading-reloading path decreases the plateau gradient by 0.07% on average, but the coefficient is not significant ($p = 0.276$). Further, the CV of the h_p variable extracted from the curves without the unloading-reloading path is also smaller at 100% (rounded to the nearest integer percentage) which compares with a CV of 142% for curves that included this path. This suggests that the scatter in h_p (the highest of any variable in Table 4) may be much reduced when unloading from the plateau is avoided, so the practice does have an undesirable effect on the data for current research purposes. In conclusion, on the basis of this data set, it appears that the presence of an unloading-reloading path does *not* significantly influence the magnitude of the non-zero yield plateau gradient, but it is better if this practice is avoided in future experimental studies that seek to provide more conclusive data for h_p.

7. Conclusions

The findings arising from this study are based on a data set of 225 stress-strain curves for structural carbon steels that were not originally obtained for research purposes and should therefore be treated with some caution.

Table 8
Effect of an unloading-reloading path on the yield plateau gradient regression statistics. [S235JR specimens tested with (107) and without (19) an unloading-reloading path, including significance levels].

	h_p (%)		r^2 coefficient		no. data points		Sign of a_2 and level†	significance	
	with	without	with	without	with	without		with	without
Mean	0.21	0.15	0.53	0.37	328	1270	+ & not	14	1
Median	0.20	0.14	0.63	0.36	244	1366	+ & 5%	6	0
Min	-1.09	-0.08	0.0003	0.0002	5	559	+ & 1%	9	0
Max	1.57	0.58	0.98	0.89	1422	1860	+ & 0.1%	71	14
CV (%)	142	100	54	80	106	31	–& 0.1%	7	4

† e.g. "+ & 1% " reports that 9 curves with the unloading-reloading path and 0 curves without it exhibited positive (+) yield plateau gradients at the 99% significance level

- Current design provisions for stocky structural members (EN 1993-1-1) and other structures (e.g. EN 1993-1-6) cannot be justified by calculation unless a finite post-yield strain-hardening tangent modulus can be guaranteed for the steel. Where true strain hardening is preceded by a significantly long yield plateau with a tangent modulus of zero, the current design provisions also cannot be justified.
- A simple nonlinear elastic-plastic finite element calculation has been used to illustrate the fact that only a very modest amount of strain hardening that begins immediately after first yield is sufficient to achieve the full plastic resistance in stocky hollow circular sections at experimentally-supported values of cross-section slenderness under the example load cases of uniform axial compression and global bending. The modest strain-hardening need only be of the order of 0.3% or less of the nominal elastic modulus, perhaps less.
- The results of 225 tensile test stress-strain curves have been extensively analysed to explore the possibility that the yield plateau has a systematic positive slope, corresponding to the modest amounts of strain hardening required as identified by the finite element calculation. The yield plateaus were first identified and isolated using a preliminary multi-part fitted algebraic characterisation. Each plateau was subsequently analysed using least squares linear regression to extract the magnitude of its mean plateau gradient (tangent modulus) and test it for statistical significance. A simple sensitivity study to variance inflation through possible autocorrelation revealed that the levels of statistical significance broadly persist even at high levels of inflation.
- Of the 225 stress-strain curves, 195 (86.7%) exhibited a yield plateau with a positive gradient, and 175 (77.8%) satisfied the 95% statistical significance level. The mean gradient of the plateau was found to be approximately 0.3% of the nominal elastic modulus, in surprisingly close agreement with the finite element calculation.
- A small group of 17 curves (7.6%) were found to have a negative yield plateau gradient satisfying the 95% significance level, averaging at approximately −0.2% of the nominal elastic modulus. This was attributed to errors in the testing process.
- A more complete statistical treatment, considering the data set as 'centred and lumped', has indicated that the steel grade has a statistically significant influence on the plateau gradient, and that the gradient should be positive for all studied steel grades.
- The presence of a statistically significant positive plateau gradient was found to be retained when the specimen was unloaded and reloaded part way along the plateau to evaluate the elastic modulus, but this practice does increase the scatter and variance in the variables. It is suggested that this practice is avoided in experimental studies that seek an accurate characterisation of the plateau gradient.
- The strain-related variables defining the hardening moduli and ductility were found to consistently exhibit higher standard errors and coefficients of variation than the stress variables of yield and ultimate strengths. While this may reflect the greater difficulty in accurately measuring strains, it also suggests that the parameters exhibit an intrinsically greater statistical variability.
- A typical stress-strain curve contains significantly more useful information than is commonly reported. The authors strongly encourage the structural engineering research community to revisit existing tensile test data sets and to explore them using a methodology akin to the

one suggested in this paper, with a view to reproducing and verifying the findings presented here.
- A carefully-conducted test programme to definitively characterise and propose bounds on the post-yield properties of the most common structural steels is greatly overdue.

Acknowledgements

This work was partly funded by the UK Engineering and Physical Sciences Research Council (EPSRC) with grant contract EP/N024060/1. The data used for this study is restricted.

References

[1] J.F. Baker, M.R. Horne, J. Heyman, The Steel Skeleton Vol. II Plastic Behaviour and Design, Cambridge University Press, Cambridge, UK, 1956.
[2] J.M. Rotter, Shell buckling design and assessment and the LBA-MNA methodology, Stahlbau 80 (11) (2011) 791–803.
[3] J.M. Rotter, The new framework for shell buckling design and the European Shell Buckling Recommendations 5th edition, ASME J. Press. Vessel. Technol. 133 (1) (2011) (011203-1 to -9).
[4] C. Doerich, J.M. Rotter, Generalised capacity curves for stability and plasticity: application and limitations, Thin-Walled Struct. 49 (2011) 1132–1140.
[5] J.M. Rotter, the new method of reference resistance design for shell structures, Proc. SDSS 2016, International Colloquium on Stability and Ductility of Steel Structures 2016, pp. 623–630 Timisoara, Romania.
[6] J.M. Rotter, Advances in understanding shell buckling phenomena and their characterisation for practical design, in: M.A. Gizejowski, A. Kowlowski, J. Marcinowski, J. Ziolko (Eds.), Recent Progress in Steel and Composite Structures, CRC Press, Taylor and Francis, London 2016, pp. 2–15.
[7] L. Gardner, The continuous strength method, Proc. ICE 161 (SB3) (2008) 127–133.
[8] L. Gardner, L. Macorini, M. Kucukler, The continuous strength method for steel and composite design, Proc. ICE 166 (SB8) (2013) 434–443.
[9] E.O. Hall, Yield Point Phenomena in Metals and Alloys, Macmillan, London, 1970.
[10] W.D. Callister Jr., Materials Science and Engineering - An Introduction, sixth ed. John Wiley & Sons, 2003.
[11] SINTAP, Assessment of the occurrence and significance of yield plateaus in structural steels, Contribution to Sub-Task 2.3 Report, Structural Integrity Assessment Procedures for European Industry (SINTAP), Brite-Euram Project N. BE95-1426, British Steel PLC, UK, 1998.
[12] EN 1993-1-5, Eurocode 3: Design of Steel Structures – Part 1–5: Plated Structural Elements, Comité Européen de Normalisation, Brussels, 2006.
[13] B.G. Neal, The Plastic Methods of Structural Analysis, third ed. Wiley & Sons, USA, 1977 1st Ed. in 1956.
[14] P. Boeraeve, B. Lognard, J. Janss, J.C. Gérardy, J.B. Schleich, Elasto-plastic behaviour of steel frame works, J. Constr. Steel Res. 27 (1993) 3–21.
[15] J.M. Rotter, A.M. Gresnigt, Material assumptions, in: J.M. Rotter, H. Schmidt (Eds.), Chapter 5 of Buckling of Steel Shells European Design Recommendations, fifth ed.European Convention for Constructional Steelwork, Brussels, 2008.
[16] A.J. Sadowski, J.M. Rotter, T. Reinke, T. Ummenhofer, Statistical analysis of the material properties of selected structural carbon steels, Struct. Saf. 53 (2015) 26–35.
[17] ABAQUS, "ABAQUS 6.14-2" Commercial FE Software, Dassault Systèmes, Simulia Corporation, Providence, RI, USA, 2014.
[18] A.J. Sadowski, J.M. Rotter, Solid or shell finite elements to model thick cylindrical tubes and shells under global bending, Int. J. Mech. Sci. 74 (2013) 143–153.
[19] J.M. Rotter, A.J. Sadowski, L. Chen, Nonlinear stability of thin elastic cylinders of different length under global bending, Int. J. Solids Struct. 51 (2014) 2826–2839.
[20] H. Schmidt, Dickwandige Kreiszylinderschalen aus Stahl unter Axialdruckbelastung, Stahlbau 58 (1989) 143–148.
[21] EN 1993-1-7, Eurocode 3: Design of Steel Structures – Part 1–6: Strength and Stability of Shell Structures, Comité Européen de Normalisation, Brussels, 2007.
[22] G. Sedlacek, et al., "Consistency of the Equivalent Geometric Imperfections Used in Design and the Tolerances for Geometric Imperfections Used in Execution" Document CEN/TC250 – CEN/TC135 – Liaison February 2010, Comité Européen de Normalisation, Brussels, 2010.
[23] ISO 6892-1, Metallic Materials – Tensile Testing – Part 1: Method of Test at Room Temperature, International Organisation for Standardisation, Geneva, 2009.
[24] X. Guo, Y. Zhang, Z. Xiong, Y. Xiang, Load-bearing capacity of occlusive high-strength steel connections, J. Constr. Steel Res. 127 (2016) 1–14.
[25] D. Vasilikis, S.A. Karamanos, S.H.J. van Es, A.M. Gresnigt, Ultimate Bending Capacity of Spiral-welded Steel Tubes – Part II: Predictions, Thin-Walled Struct. 102 (2016) 305–319.
[26] G. Xiong, S.-B. Kang, B. Yang, S. Wang, J. Bai, S. Nie, Y. Hu, G. Dai, Experimental and numerical studies on lateral torsional buckling of welded Q460GJ structural steel beams, Eng. Struct. 126 (2016) 1–14.
[27] JCSS, Probabilistic Model Code – 12th draft, JCSS-OSTL/DIA/VROU-10-11-2000, Joint Committee on Structural Safety, 2001 Accessed on 11/02/14, available at: http://www.jcss.byg.dtu.dk/Publications/Probabilistic_Model_Code.aspx.
[28] EN 10027-1, Designation Systems for Steels – Part 1: Steel Names, Comité Européen de Normalisation, Brussels, 2005.
[29] EN 10027-2, Designation Systems for Steels – Part 2: Steel Numbers, Comité Européen de Normalisation, Brussels, 1992.
[30] A.J. Sadowski, J.M. Rotter, T. Reinke, T. Ummenhofer, Analysis of variance of tensile tests from spiral welded carbon steel tubes, Constr. Build. Mater. 75 (2015) 208–212.
[31] S.H.J. van Es, A.M. Gresnigt, D. Vasilikis, S. Karamanos, Ultimate bending capacity of spiral-welded steel tubes – part I: experiments, Thin-Walled Struct. 102 (2016) 286–304.
[32] Mathworks, Matlab Release 2014a, 2014 (Natick, MA, USA).
[33] C. Petersen, Stahlbau: Grundlagen der Berechnung und baulichen Ausbildung von Stahlbauten – 3. Überarbeitete und erweiterte Auflage, Vieweg, Braunschweig, 1993.
[34] J. Fox, Regression diagnostics, Sage University Paper Series on Quantitative Applications in the Social Sciences, N. 07-079, 1991 (Newbury Park, CA).
[35] C.W. Ostrom, Time series analysis: regression techniques, Sage University Paper Series on Quantitative Applications in the Social Sciences, N. 07-009, second ed., 1978 (Newbury Park, CA).
[36] G. Ljung, G.E.P. Box, On a measure of lack of fit in time series models, Biometrika 66 (1978) 67–72.
[37] A.M. Law, W.D. Kelton, Simulation Modelling and Analysis, second ed. McGraw-Hill, 1991 284.